CHEMISTRY
A EUROPEAN JOURNAL

DOI: 10.1002/chem.200501284

Electronic Properties and Reactivity of Short-Chain Oligomers of 3,4-Phenylenedioxythiophene (PheDOT)

Igor F. Perepichka,*[a, b] Sophie Roquet,[a] Philippe Leriche,*[a] Jean-Manuel Raimundo,[a, c] Pierre Frère,[a] and Jean Roncali*[a]

Abstract: The dimer and trimer of 3,4-phenylenedioxythiophene (PheDOT) have been synthesized. Unlike the parent systems based on 3,4-ethylenedioxythiophene (EDOT), these compounds are quite stable under atmospheric conditions. The electronic absorption spectra of di- and tri-PheDOT exhibit a well-resolved vibronic fine structure indicative of self-rigidification of the conjugated structure by noncovalent intramolecular sulfur–oxygen interactions. Comparison of UV-visible data for the PheDOT oligomers with those of the corresponding EDOT oligomers reveals a faster decrease of the HOMO–LUMO gap with chain length for the former. Cyclic voltammetric data show that whereas PheDOT oxidizes at a lower potential than EDOT, the PheDOT dimer and trimer exhibit much higher oxidation potentials than their EDOT-based analogues. A comparative analysis of the electropolymerization of the three PheDOT-based systems shows that although PheDOT is very difficult to polymerize, its dimer and trimer can be readily electropolymerized. This unexpected increase of reactivity with chain extension is discussed with the aid of theoretical calculations.

Keywords: conjugation · electrochemistry · oligomers · polymerization · structure–property relationships

Introduction

In the past decade, 3,4-ethylenedioxythiophene (EDOT) has generated considerable interest not only as the monomer of the well-known poly(EDOT) widely used because of its unique combination of conductivity, stability, and optical transparency,[1] but also as a building block for the development of various classes of functional π-conjugated systems.[2–4] In addition to its wide use for the design of functional or low-band-gap conducting polymers,[2–4] EDOT has also been employed as a building block for the synthesis of various classes of molecular π-conjugated systems including fluorophores,[5] nonlinear optical (NLO)-phores,[6] extended tetrathiafulvalene analogues,[7] and π-conjugated oligomers.[8]

It has been shown already that in addition to their electron-donor properties and the prevention of defective α–β′ couplings during polymerization, the oxygen atoms at the 3- and 4-positions of the thiophene ring induce a self-structuration of the π-conjugated chain by noncovalent intramolecular sulfur–oxygen interactions.[4] However, a counterpart of these positive effects is that the synthesis of soluble poly(EDOT) derivatives implies the substitution of an sp^3-carbon atom of the ethylenedioxy bridge, which has undesirable consequences, namely, 1) the creation of a stereogenic center, which will generate regio- and stereoisomers in the resulting oligomers or polymers and 2) the noncoplanarity of the substituent and π-conjugated system, which will increase interchain distances and thus lead to an alteration of the charge-transport properties of the resulting solid-state material.

[a] Dr. I. F. Perepichka, Dr. S. Roquet, Dr. P. Leriche, Dr. J.-M. Raimundo, Prof. P. Frère, Dr. J. Roncali
Groupe Systèmes Conjugués Linéaires
CIMMA, UMR 6200 CNRS, Université d'Angers
2 Boulevard Lavoisier, 49045 Angers (France)
Fax: (+33) 241-735-405
E-mail: philippe.Leriche@univ-angers.fr
Jean.Roncali@univ-angers.fr

[b] Dr. I. F. Perepichka
LM Litvinenko Institute for Physical Organic and Coal Chemistry of the National Academy of Science of Ukraine
Donetsk, 83114 (Ukraine)
Current address:
Department of Chemistry
University of Durham, Durham DH1 3LE (UK)
Fax: (+44) 191-384-4737
E-mail: i.f.perepichka@durham.ac.uk

[c] Dr. J.-M. Raimundo
CMOM, Faculté des Sciences
Université de Nice SophiaAntipolis
28 Avenue Valrose, 06108 Nice (France)

WILEY InterScience DISCOVER SOMETHING GREAT
© 2006 Wiley-VCH Verlag GmbH & Co. KGaA, Weinheim

In an attempt to solve this problem, we recently reported the synthesis of 3,4-phenylenedioxythiophene (**1-P**) in which the ethylene bridge of EDOT (**1-E**) is replaced by a 1,2-phenylene moiety thus allowing further coplanar substitution at the sp^2-carbon atoms of the benzene ring.[9] However, as shown by experimental and theoretical results, the stabilization of the cation radical resulting from the introduction of a phenyl ring renders the polymerization of PheDOT very difficult. In spite of this drawback, PheDOT remains an attractive building block for the design and synthesis of soluble π-conjugated systems combining the donor and self-structuring properties inherent in the EDOT unit with possible compact π stacking in the solid state. As a first step in the exploration of the potentialities of PheDOT in the design of functional π-conjugated systems, we report here the synthesis of the PheDOT dimer (**2-P**) and trimer (**3-P**) and the characterization of their electronic properties by means of UV-visible spectroscopy and cyclic voltammetry experiments. The electrochemical polymerization of these compounds has been investigated and the chain-length dependence of their reactivity is discussed with the aid of theoretical calculations.

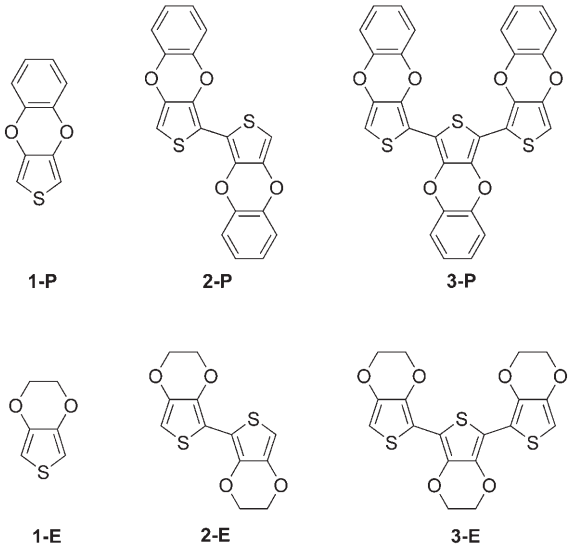

Results and Discussion

The synthesis of **2-P** and **3-P** is depicted in Scheme 1. PheDOT (**1-P**) was synthesized as already reported.[9] Treatment of **1-P** with butyllithium in THF at −70 °C followed by oxidative coupling of the lithiated derivative of **1-P** with $CuCl_2$ gave dimer **2-P** in a 73 % yield. Treatment of **1-P** with NBS in DMF at room temperature and in the absence of light gave 2,5-dibromo-PheDOT (**4**) in an 85 % yield. Reaction of the lithiated derivative of PheDOT with a solution of anhydrous zinc chloride in THF led to the formation of zinc derivative **5**, which was immediately reacted with **4** in the presence of $[Pd(PPh_3)_4]$ to give compound **3-P** in a 21 % yield. Contrary to the EDOT trimer (**3-E**),[10] **3-P** is stable for days under atmospheric conditions.

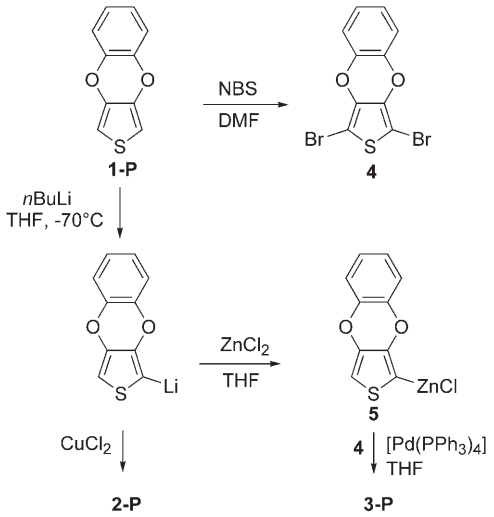

Scheme 1.

Wudl and co-workers have shown that highly conducting poly(EDOT) can be readily obtained by solid-state polymerization of 2,5-dibromo-EDOT at room temperature.[11] On this basis, we have investigated the possible solid-state polymerization of 2,5-dibromo-PheDOT (**4**). Surprisingly, we found that compound **4** is quite stable and does not show any decomposition even after storage above 100 °C for one month.

Figure 1 shows the crystallographic structure of compound **4**. As expected, the PheDOT system is perfectly planar. In particular, the side view clearly shows that the slight deviation from planarity found in the ethylene bridge of EDOT is eliminated when this bridge is replaced by a phenylene one. On the other hand, examination of the crystal-packing diagram of compound **4** shows that the molecules adopt a head-to-tail placement with Br···Br distances of 4.47 Å. This value is larger than the sum of the van der Waals radii (3.90 Å) and much larger than that found in the dibromo-EDOT crystal (3.45 Å).[11] This considerable difference in the Br···Br distance could explain the absence of polymerization for compound **4**.

Figure 2 shows the UV-visible absorption spectra of compounds **1-P**, **2-P**, and **3-P**. As already observed for EDOT oligomers, the spectra of **2-P** and **3-P** exhibit a well-resolved vibronic fine structure with three maxima equally spaced by 1300–1400 cm^{-1} corresponding to the coupling of the C=C stretching mode with the electronic structure.[12] Such spectral features are typical for planar, rigid conjugated systems. As demonstrated by crystallographic data of various classes of EDOT-based π-conjugated systems, this rigidity arises from noncovalent intramolecular S···O interactions.[4,6,8]

Comparison of the UV-visible data for the EDOT and PheDOT series shows that whereas the absorption maximum (λ_{max}) of PheDOT **1-P** (274 nm) is redshifted relative to EDOT (261 nm) the situation is inverted for longer systems, and compounds **2-P** and **3-P** show absorption maxima at shorter wavelengths than their EDOT analogues. Com-

 © 2006 Wiley-VCH Verlag GmbH & Co. KGaA, Weinheim

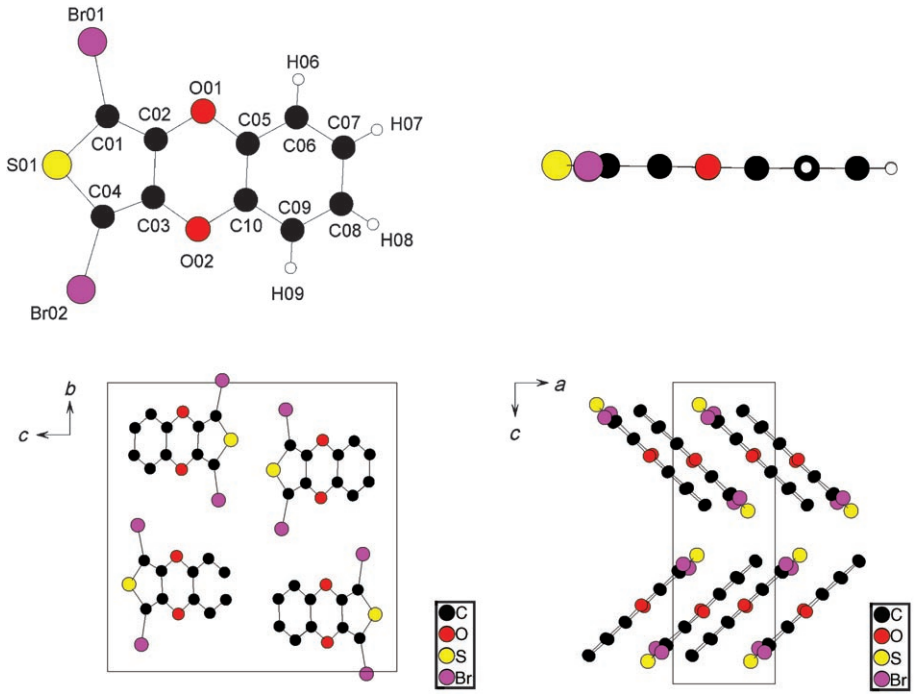

Figure 1. Crystallographic structure of dibromo-PheDOT **4**.

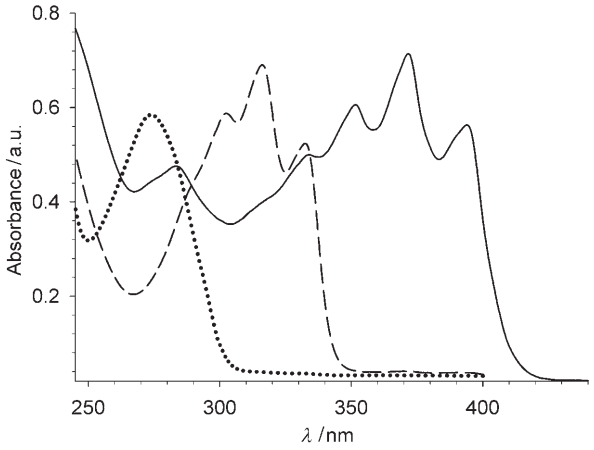

Figure 2. UV/Vis absorption spectra of **1-P** (•••••), **2-P** (– – –), and **3-P** (——) in CH_2Cl_2.

parison of the width of the HOMO–LUMO gap (ΔE) estimated from λ_{max} values shows that whereas ΔE decreases by 0.22 eV between EDOT and PheDOT it increases by 0.06 eV between **2-E** and **2-P** and by 0.23 eV between **3-E** and **3-P** (Table 1). Thus, except for the monomer, replacement of the ethylenedioxy bridge by a phenylenedioxy one leads to an increase of the HOMO–LUMO gap of the corresponding oligomers.

The oxidation potentials of the six compounds have been determined by cyclic voltammetry (CV) in dichloromethane in the presence of tetrabutylammonium as the supporting electrolyte. The single-scan cyclic voltammogram of a solution of PheDOT shows an irreversible anodic peak at a potential (E_{pa}) of 1.48 V versus Ag/AgCl, a value 20 mV higher than that observed for EDOT under the same conditions.

Comparison of the CV data for the dimers and trimers shows that for **2-P** the E_{pa} value is 0.36 V higher than that for **2-E**, whereas this difference amounts to 0.43 V between **3-P** and **3-E**. Examination of these data together with UV-visible results shows that the decrease of the HOMO level suggested by the E_{pa} values is much larger than the corresponding increase of ΔE indicated by the optical data. This discrepancy thus suggests that the decrease of the HOMO level with successive chain extension is accompanied by a concomitant but smaller decrease of the LUMO level.

To gain more detailed information on these points, ab initio calculations on the EDOT and PheDOT oligomers up to the tetramer stage have been performed by using the density functional theory (DFT) method. In DFT calculations we employed the B3LYP hybrid density functional[13,14] with Pople's triple-split valence basis set supplemented by polarization functions on heavy atoms (2d) and hydrogen atoms (p) (B3LYP/6-311G(2d,p)) for both full-geometry optimization and electronic-structure calculations.

Table 1. Anodic peak potentials[a] and UV/Vis absorption[b] data for PheDOT and EDOT compounds.

Compound	E_{pa} [V]	λ_{max} [nm]	ΔE [eV]
1-E	1.50	261	4.75
2-E	0.84	322	3.85
3-E	0.49	400	3.10
1-P	1.48	274	4.53
2-P	1.20	317	3.91
3-P	0.92	372	3.33

[a] Recorded in 0.10 M Bu_4NPF_6/CH_2Cl_2, scan rate 100 mV s^{-1}, reference Ag/AgCl. [b] Recorded in CH_2Cl_2.

Table 2 lists the results obtained for the two series of oligomers. As expected, the optimized geometry of all oligomers exhibits a planar *anti* conformation. The calculated nonbonded sulfur–oxygen distances of 2.91 and 2.95 Å for EDOT and PheDOT oligomers, respectively, are clearly smaller than the sum of the van der Waals radii of the two atoms (1.80 + 1.52 = 3.32 Å) and close to the distances observed for the crystallographic structures of various conjugated systems incorporating EDOT units.[4,6–8] For **1-E** and **1-P**, the C(3) and C(4) atoms of the thiophene ring present substantial HOMO coefficients and form bonding MOs (Figure 3). However, for **1-P**, the HOMO is also delocalized

 © 2006 Wiley-VCH Verlag GmbH & Co. KGaA, Weinheim

Table 2. HOMO and LUMO energy levels [eV] of the EDOT and PheDOT compounds.

Compound	HOMO	LUMO	ΔE
1-E	−5.93	−0.23	5.70
2-E	−5.04	−0.95	4.09
3-E	−4.59	−1.27	3.32
4-E	−4.34	−1.44	2.91
1-P	−5.68	−0.51	5.17
2-P	−5.50	−1.38	4.12
3-P	−5.18	−1.74	3.44
4-P	−4.99	−1.93	3.06

over the benzene ring and contrary to EDOT, population on the C(2) and C(5) atoms of thiophene is negligible. Comparison of the HOMO for the longer systems of the two series reveals a quite different situation because for these PheDOT oligomers the HOMO no longer populates the benzene ring but becomes progressively similar to that of EDOT oligomers and at the tetramer stage the two oligomers show identical HOMO distribution.

For both series of oligomers, the LUMO is essentially located on the thiophenic backbone and the high coefficients on the exocyclic C(2)-C(2′) interthiophene bonds are in agreement with a quinonoid structure. The results in Table 2 show that except for **1-P**, which presents a higher HOMO level and a smaller ΔE value than **1-E**, PheDOT oligomers have lower HOMO and LUMO levels and larger HOMO–LUMO gaps than their EDOT analogues.

Examination of the calculated bond lengths for the two series shows that the distance between the carbon atoms of the 3- and 4-positions of the thiophene ring and the oxygen atoms ($O{-}C_{Th}$) are longer for the $(PheDOT)_n$ compounds ($\approx$1.37 Å) than for the $(EDOT)_n$ compounds (1.35–1.36 Å). Conversely, the bonds between the oxygen and the carbon atoms of the phenylene and bridge ($O{-}C_{Ph}$) of $(PheDOT)_n$ compounds (1.38–1.39 Å) are shorter than the bonds between the oxygen and carbon atoms of the ethylene bridge ($O{-}C_{Alk}$, $\approx$1.43 Å). These differences suggest that replacement of the ethylene bridge by a phenylene one leads to a decrease of the electron-releasing mesomeric effect of the ether group in the PheDOT system. For the monomer this effect is counterbalanced by the electron delocalization over the whole molecule, which explains the lower HOMO–LUMO gap relative to EDOT. However, for longer systems the combined effects of the preferential electron delocalization along the poly(thiophene) backbone and the smaller electron-donor effect of the ether groups result in a parallel increase of the HOMO and LUMO levels.

Figure 4 shows the variation of the HOMO and LUMO level as a function of the reciprocal number of thiophene units (n) in the conjugated chain for the two series of oligomers. For EDOT oligomers the HOMO and LUMO levels vary linearly with $1/n$ as reported for many series of π-conjugated oligomers.[15] A linear variation of the LUMO level versus $1/n$ is also found for PheDOT oligomers, however, for the HOMO, the point corresponding to the **1-P** monomer is located above the line, for the already discussed reasons. Although the LUMO level increases faster for PheDOT oligomers, the slower increase of the HOMO level results in a smaller overall reduction of the HOMO–LUMO gap with chain extension. Extrapolation of the two lines to an infinite chain length leads to a predicted band gap of 2.12 eV for poly(PheDOT) and 2.10 eV for poly(EDOT), in

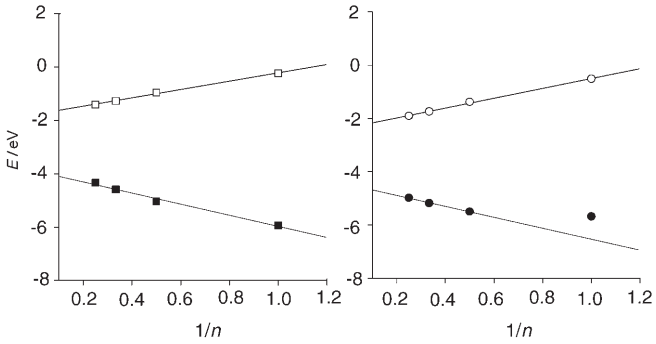

Figure 4. Variation of the HOMO (■/●) and LUMO (□/○) levels for $(EDOT)_n$ (left) and $(PheDOT)_n$ compounds (right) versus the reciprocal number of thiophene units in the conjugated chain.

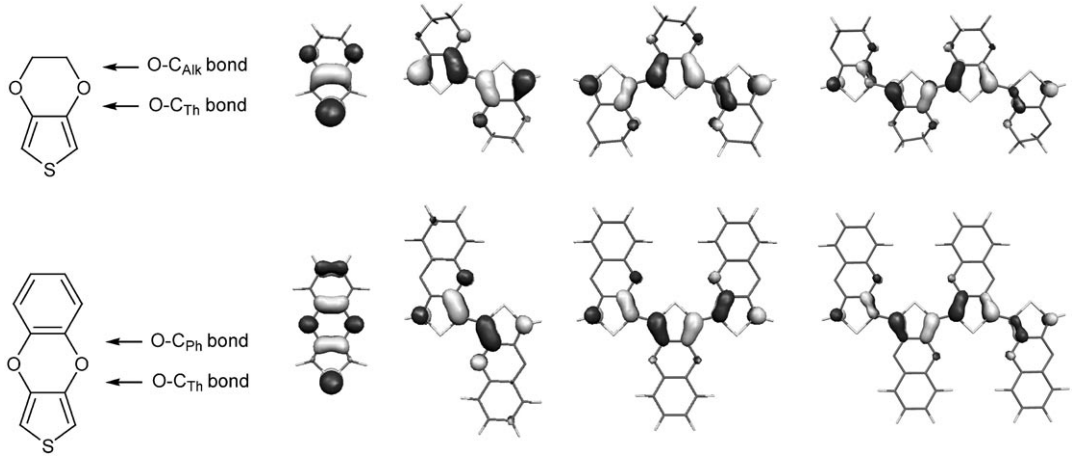

Figure 3. HOMO orbitals of EDOT (top) and PheDOT (bottom) oligomers (B3LYP/6-311G(2d,p)).

 © 2006 Wiley-VCH Verlag GmbH & Co. KGaA, Weinheim

qualitative agreement with previous experimental results[9] and with the above-mentioned UV-visible data (Table 1).

It has been known for a long time that the chain extension of π-conjugated oligomers leads to a decrease in the reactivity of the corresponding cation radical.[16] Because of the delocalization of the cation radical over the whole π-conjugated system, the density of an unpaired electron at the terminal coupling position decreases making polymerization less and less efficient as the chain length of the precursor increases.[16,17] In a previous study we have shown that for PheDOT, delocalization of the cation radical over the whole molecule strongly decreases its reactivity thus making the electropolymerization process difficult and not very efficient.[9] In this context, longer PheDOT oligomers were not expected to give rise to any electropolymerization.

Contrary to what could be expected, application of recurrent potential scans to a 3×10^{-3} M solution of **2-P** in dichloromethane leads to the rapid development of a broad redox system extending from −0.2 to +1.00 V indicating a straightforward polymerization (Figure 5). Owing to the very low solubility of **3-P**, electropolymerization was carried out in nitrobenzene with a maximum substrate concentration of 1×10^{-4} M. Nevertheless, in this case too, application of repetitive potential scans produces the emergence of a new redox system with a narrow anodic wave peaking at 0.65 V and a cathodic peak at 0.40 V (Figure 5).

Figure 6 shows the CV data of poly(**2-P**) and poly(**3-P**) recorded in a monomer-free electrolytic medium. Whereas, as already reported, the cyclic voltammogram of poly(PheDOT) exhibits a broad and structureless redox system extending from −0.20 to +1.20 V (see Figure 3 in ref. [9]), those of the polymers derived from the dimer and trimer show well-defined redox systems with anodic waves peaking at 0.40 and 0.29 V for poly(**2-P**) and poly(**3-P**), respectively. This 110 mV negative shift of the anodic peak for poly(**3-P**) suggests a longer effective conjugation length than that for poly(**2-P**) and even more so than that for poly(**1-P**).

Thus, the progressive improvement of the resolution of the CV data and the negative shift of the anodic peak potential from poly(**1-P**) to poly(**3-P**) suggests that in sharp contrast to what has been observed for oligothiophenes,[17,18] the use of the dimer and trimer as precursor allows the synthesis of better-defined and more-extensively-conjugated polymers.

Some information concerning the chain-length dependence of the reactivity of the various precursors was provided by examination of the singly occupied molecular orbital (SOMO) of the cation radical from the monomer to the tetramer for the two series of precursors. Whereas for the two series the SOMO energy increases with chain length, the energy difference between the monomer and the tetramer is larger for the EDOT series (−11.53 and −7.45 eV for **1-E** and **4-E**, respectively, versus −10.70 and −7.83 eV for **1-P** and **4-P**, respectively).

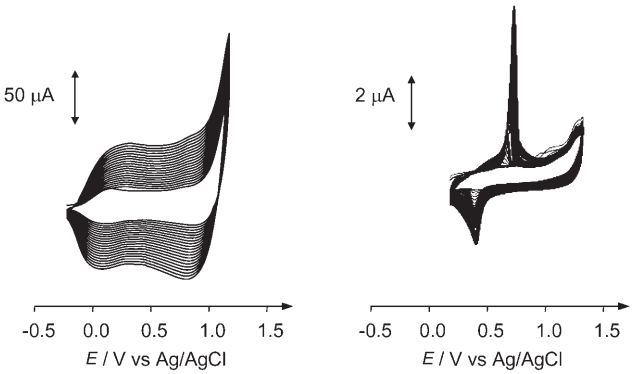

Figure 5. Potentiodynamic electropolymerization of **2-P** (3×10^{-3} M) in 0.20 M Bu_4NPF_6/CH_2Cl_2 with a scan rate of 100 mV s^{-1} (left); **3-P** (1×10^{-4} M) in 0.20 M Bu_4NPF_6/nitrobenzene with a scan rate of 100 mV s^{-1} (right).

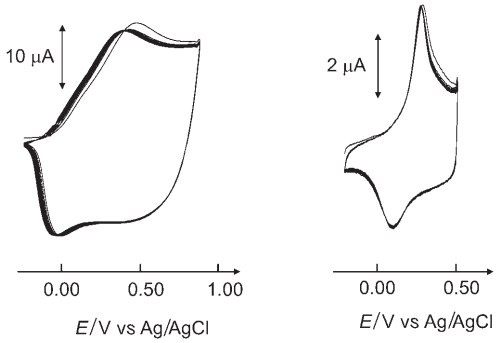

Figure 6. Cyclic voltammograms of poly(**2-P**) (left) and poly(**3-P**) (right) (prepared under the same conditions as those given in Figure 5) in 0.20 M Bu_4NPF_6/MeCN with a scan rate of 100 mV s^{-1}.

Figure 7 shows the α-SOMO orbitals for the radical cations of the EDOT and PheDOT series. As previously under-

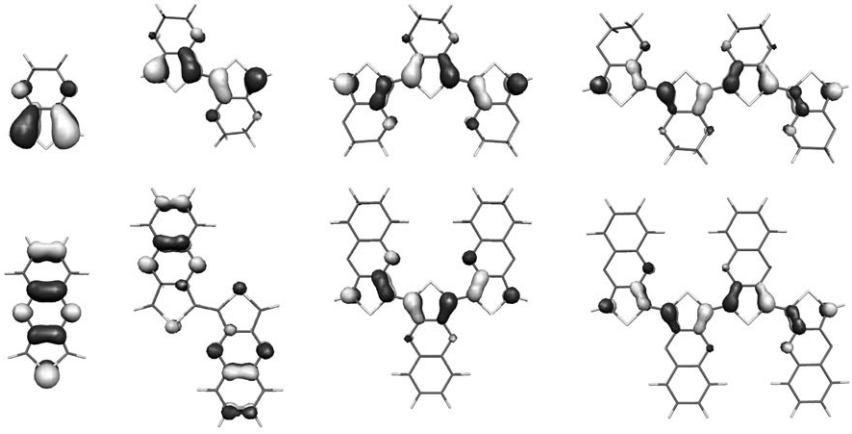

Figure 7. SOMOs of $(EDOT)_n$ (top) and $(PheDOT)_n$ compounds (bottom).

© 2006 Wiley-VCH Verlag GmbH & Co. KGaA, Weinheim

lined, the presence of null coefficients on the C(2) and C(5) positions of the PheDOT cation radical explains its poor reactivity compared with the EDOT cation radical.[9] However, chain extension leads to a more homogeneous distribution of the SOMO coefficients and at the trimer stage, the SOMO of **3-P** is delocalized along the whole of the conjugated backbone forming bonding C(2)–C(3) orbitals with substantial coefficients at the terminal α-carbon atoms of the thiophene rings. The SOMO no longer populates the benzene ring and only small coefficients are observed on the inner oxygen atoms of the two lateral monomer units, similarly to the EDOT trimer. Finally, calculations predict that at the tetramer stage the terminal α-thiophene positions should present practically the same reactivity for the two series. These results are consistent with the similarity found in the HOMO distribution of the two systems. However, it remains that the overall reactivity decreases with chain extension due to the stabilization of the cation radical. Consequently, chain extension of the PheDOT oligomers lead to counteracting effects, namely, the phenyl group which strongly contributes to limiting the reactivity of the PheDOT cation radical has less effect thus allowing a more efficient polymerization of the PheDOT dimer and trimer. On the other hand, the decrease of reactivity of the cation radical and of the solubility will necessarily limit the polymerizability of highly extended systems. In this context, the above-mentioned electrochemical results suggest that the trimer of PheDOT may represent an optimum trade-off between reactivity and solubility.

Conclusion

To summarize, short-chain PheDOT oligomers have been synthesized. UV-visible absorption spectra have shown that the self-rigidification of the conjugated structure by noncovalent intramolecular sulfur–oxygen interactions widely observed in EDOT-containing conjugated systems are still present in PheDOT-based systems. Optical and electrochemical data have shown that whereas PheDOT has a lower oxidation potential and a smaller HOMO–LUMO gap than EDOT, the PheDOT dimer and trimer show higher oxidation potentials and larger HOMO–LUMO gaps than their EDOT analogues. Theoretical results obtained for oligomers up to the tetramer stage extrapolated to an infinite polymer chain length leads to predicted band gaps that are larger for poly(PheDOT) than for poly(EDOT), in agreement with experimental results.

The electrochemical polymerization of the PheDOT dimer and trimer has been investigated. In spite of the very low substrate concentration imposed by their low solubility, both compounds undergo a straightforward polymerization. The cyclic voltammetric data of the obtained polymers suggest that the increase of the chain length of the precursor to the trimer stage leads to an enhancement of the effective conjugation length of the resulting polymer Theoretical calculations carried out to interpret this surprising result show that whereas the cation radical of PheDOT is not very reactive due to the delocalization of the unpaired electron over the whole molecule, extension of the conjugated chain to the dimer and trimer leads to a distribution of the SOMO which becomes progressively similar to that of EDOT oligomers. The significantly lower HOMO level of PheDOT oligomers compared with their EDOT analogues thus opens the possibility to synthesize π-conjugated systems stable in ambient conditions and which can be solubilized by appropriate alkyl chains while preserving the compact packing organization needed to ensure high charge-carrier mobility. Work in this direction is now underway and will be reported in future publications.

Experimental Section

General: ^{1}H and ^{13}C NMR spectra were recorded on Bruker Avance DRX 500 (500 MHz), Bruker Avance DRX 400 (400 MHz), and Varian Unity 300 (300 MHz) instruments, using tetramethylsilane as internal standard (in some cases spectra were referred to the solvent as internal standard). Mass spectra were recorded on a VG7070E spectrometer operating at 70 eV (EI), a Bruker Biflex-III (MALDI-TOF) and a JEOL LMS700 (HRMS). UV/Vis-NIR spectra were recorded on Perkin–Elmer Lambda 19 NIR or Varian Cary 5E spectrophotometers.

2,5-Dibromo-3,4-(1,2-phenylenedioxy)thiophene (4): 3,4-(1,2-Phenylenedioxy)thiophene (**1**: 2.00 g, 10.5 mmol) was dissolved in dry *N*,*N*-dimethylformamide (DMF: 35 mL) under nitrogen. *N*-Bromosuccinimide (NBS: 4.0 g, 22.5 mmol) was added in one portion and the mixture was stirred at room temperature for 2 h (protected from daylight). Precipitation (colorless crystals) was observed in 45 min. The mixture was cooled to 0 °C, kept for 30 min, filtered off, and then washed with cold DMF and water yielding pure compound **4** (2.69 g, 73.5 %; m.p. 153–154 °C) as white crystals. Dilution of the DMF filtrate with water gave an additional portion of product **4** (0.78 g, 21.3 %). ^{1}H NMR (500 MHz, $CDCl_3$): δ = 7.01–7.04 (m, 2H), 6.97–7.00 ppm (m, 2H); ^{13}C NMR (125 MHz, $CDCl_3$): 139.82, 137.32, 124.37, 117.00, 86.98 ppm; MS (EI): *m*/*z* (%): 349.7, 347.7, 345.7 (50, 100, 50) [M^+]; calcd exact mass: 345.82987; elemental analysis calcd (%) for $C_{10}H_4Br_2O_2S$ (M_r = 348.01): C 34.51, H 1.16, Br 45.92, S 9.21; found: C 34.60, H 1.13, Br 45.75, S 9.35.

2,2′-Bis[3,4-(1,2-phenylenedioxy)thienyl] (2-P): Under nitrogen, *n*BuLi (1.6 M in hexane, 1.35 mL, 2.16 mmol) was added dropwise to a solution of PheDOT **1** (400 mg, 2.10 mmol) in dry THF (10 mL) at −70 °C. The mixture was allowed to warm slowly to 0 °C and stirred at this temperature for 40 min. It was cooled to −30 °C, dry $CuCl_2$ (300 mg, 2.23 mmol) was added, and the mixture was stirred at room temperature for 16 h. The mixture was diluted with water and extracted with CH_2Cl_2. The organic layer was slightly acidified by using diluted HCl, washed with water, and dried over $MgSO_4$. Evaporation of the solvent and flash chromatography of the residue on silica gel (petroleum ether/CH_2Cl_2, 1:1 v/v) afforded compound **2** (285 mg, 73 %) as a colorless (slightly greyish) solid. M.p. 280.5–281 °C; ^{1}H NMR (500 MHz, [D$_6$]DMSO): δ = 7.08–7.13 (m, 4H), 7.04–7.07 (m, 4H), 7.05 ppm (s, 2H); MS (MALDI TOF): *m*/*z*: 378.07 [M^+]; calcd exact mass: 378.00205; elemental analysis calcd (%) for $C_{20}H_{10}O_4S_2$ (M_r = 378.42): C 63.48, H 2.66; found: C 63.35, H 2.53.

2,2′,5′,2″-tris[3,4-(1,2-phenylenedioxy)thienylene] (3-P): Under nitrogen, *n*BuLi (2.5 M in hexane, 0.81 mL, 2.03 mmol) was added dropwise to a solution of PheDOT **1** (380 mg, 2.00 mmol) in dry THF (7 mL) at −70 °C. The mixture was allowed to warm to 0 °C for 30 min and was stirred at this temperature for an additional 30 min. This solution was added by syringe under nitrogen to a solution of anhydrous $ZnCl_2$ (0.27 g) in THF (6 mL) at −10 to 0 °C and the mixture was stirred at room temperature for 20 min. The resulting solution of zinc derivative **5** was added by syringe under nitrogen to a solution of dibromide **4** (348 mg, 1.00 mmol) and [Pd(PPh_3)$_4$] (25 mg, 0.022 mmol) in THF (5 mL) and the mixture was

 © 2006 Wiley-VCH Verlag GmbH & Co. KGaA, Weinheim

stirred at room temperature for 4 days (an additional portion of [Pd(PPh_3)$_4$] (50 mg, 0.043 mmol) was added after 12 h). The solvent was evaporated and the residue was transferred onto an extractor and extracted by refluxing CH_2Cl_2 (250 mL) for 15 h. After having passed the solution through a 4 cm layer of silica gel to separate it from the inorganic material and then precipitated it from CH_2Cl_2, the solid was filtered off affording compound **3** (120 mg, 21 %; m.p. 315–320 °C (decomp)) as yellow powder, which was barely soluble in most organic solvents. ^{1}H NMR (500 MHz, $CDCl_3$): $\delta = 7.04$–7.08 (m, 4H), 6.96–7.01 (m, 8H), 6.47 ppm (s, 2H); MS (MALDI TOF): m/z: 565.91 [M^+]; calcd exact mass: 565.99.

Computational procedure: The ab initio computations were carried out with the Gaussian 98 package of programs at a hybrid density-functional theory (DFT) level.[19] In DFT calculations, we adopted Becke's three-parameter hybrid exchange functional and the correlation functional of Lee, Yang, and Parr (B3LYP).[13,14] Calculations were performed by using Pople's 6-311G triple split valence basis set supplemented by two d-polarization functions on heavy atoms and p-polarization functions on hydrogen atoms. Geometries and electronic structures were calculated at the same B3LYP/6-311G(2d,p) level. Presentation of orbital populations was performed by using the Molekel v.4.3 program.[20] No constraints of bonds/angles/dihedral angles were applied in the calculations and all the atoms were free to optimize.

Crystal data and structure refinement for 4: empirical formula = $C_{10}H_4Br_2O_2S$; $M_r = 348.01$; $T = 293(2)$ K; $\lambda = 0.71073$ Å; crystal system: orthorhombic; space group: $P2_12_12_1$; $a = 4.9929(4)$, $b = 14.605(2)$, $c = 14.599(2)$ Å; $\alpha = \beta = \gamma = 90°$; $V = 1064.6(2)$ Å^3; $Z = 4$; $\rho_{calcd} = 2.171$ g cm^{-3}; $\mu = 7.783$ mm^{-1}; $F(000) = 664$; crystal size: $0.43 \times 0.09 \times 0.06$ mm; $\theta = 1.97$–$25.80°$; limiting indices: $-5 \le h \le 5$, $-17 \le k \le 17$, $-17 \le l \le 14$; reflections collected/unique [R(int) = 0.0462] = 6517/1968; completeness to $\theta = 25.80°$, 97.0 %; absorption correction: semiempirical from equivalents; max/min transmission = 0.2935/0.278; refinement method: full-matrix least-squares on F^2; data/restraints/parameters = 1968/0/136; GOF on $F^2 = 0.877$; final R indices [$I > 2\sigma(I)$]: $R1 = 0.0283$, $wR2 = 0.0470$; R indices (all data): $R1 = 0.0560$, $wR2 = 0.0515$; absolute structure parameter = 0.046(16); largest diff. peak/hole = 0.491/−0.278 e Å^{-3}.

CCDC-261998 contains the supplementary crystallographic data for this paper. These data can be obtained free of charge from the Cambridge Crystallographic Data Centre via www.cdc.cam.ac.uk/data_request/cif.

Acknowledgments

The authors thank the Région des Pays de la Loire for the PhD grant for S.R., and the Total company for financial support. I.F.P. thanks the "Pole de Recherche et d'Innovation d'Angers" (PRIA) for financial support of his visiting professorship at the Université d'Angers. We thank Dr. J. Delaunay (SCAS of Angers) for NMR analyses and M. Allain for X-ray determination.

[1] S. Kirchmeyer, K. Reuter, *J. Mater. Chem.* **2005**, *15*, 2077.
[2] B. L. Groenendaal, F. Jonas, D. Freitag, D. Pielartzik, J. R. Reynolds, *Adv. Mater.* **2000**, *12*, 481.
[3] J. Roncali, *J. Mater. Chem.* **1999**, *9*, 1975.
[4] J. Roncali, P. Blanchard, P. Frère, *J. Mater. Chem.* **2005**, *15*, 1589.
[5] J.-M. Raimundo, P. Blanchard, H. Brisset, S. Akoudad J. Roncali, *Chem. Commun.* **2000**, 939.
[6] a) J. M. Raimundo, P. Blanchard, P. Frère, N. Mercier, I. Ledoux Rak, R. Hierle, J. Roncali, *Tetrahedron Lett.* **2001**, *42*, 1507; b) J. M. Raimundo, P. Blanchard, N. Gallego Planas, N. Mercier, I. Ledoux Rak, R. Hierle, *J. Org. Chem.* **2002**, *67*, 205.
[7] a) S. Akoudad, P. Frère, N. Mercier, J. Roncali, *J. Org. Chem.* **1999**, *64*, 4267; b) P. Leriche, M. Turbiez, V. Monroche, P. Frère, P. Blanchard, P. J. Skabara, J. Roncali, *Tetrahedron Lett.* **2003**, *44*, 649.
[8] a) A. K. Mohanakrishnan, A. Hucke, M. A. Lyon, M. V. Lakshmikantham, M. P. Cava, *Tetrahedron* **1999**, *55*, 11745; b) M. Turbiez, P. Frère, P. Blanchard, J. Roncali, *Tetrahedron Lett.* **2000**, *41*, 5521; c) R. G. Hicks, M. B. Nodwell, *J. Am. Chem. Soc.* **2000**, *122*, 6746; d) J. J. Apperloo, L. Groenendaal, H. Verheyen, M. Jayakannan, R. A. J. Janssen, A. Dkhissi, D. Beljonne, R. Lazzaroni, J. L. Brédas, *Chem. Eur. J.* **2002**, *8*, 2384; e) M. Turbiez, P. Frère, J. Roncali, *J. Org. Chem.* **2003**, *68*, 5357; f) Turbiez, P. Frère, M. Allain, C. Videlot, J. Ackermann, J. Roncali, *Chem. Eur. J.* **2005**, *11*, 3742.
[9] S. Roquet, P. Leriche, I. F. Perepichka, B. Jousselme, P. Frère, J. Roncali, *J. Mater. Chem.* **2004**, *14*, 1396.
[10] G. A. Sotzing, J. R. Reynolds, P. J. Steel, *Chem. Mater.* **1996**, *8*, 882.
[11] H. Meng, D. F. Perepichka, F. Wudl, *Angew. Chem.* **2003**, *115*, 682; *Angew. Chem. Int. Ed.* **2003**, *42*, 658.
[12] a) S. D. D. V. Rughooputh, S. Hotta, A. J. Heeger, F. Wudl, *J. Polym. Sci. Part B* **1987**, *25*, 1071; b) O. Inganäs, W. Salaneck, J. E. Osterholm, J. Laakso, *Synth. Met.* **1988**, *22*, 395.
[13] a) A. D. Becke, *Phys. Rev. A* **1988**, *38*, 3098; b) A. D. Becke, *J. Chem. Phys.* **1993**, *98*, 5648.
[14] C. Lee, W. Yang, R. G. Parr, *Phys. Rev. B* **1988**, *37*, 785.
[15] a) P. Bäuerle, *Adv. Mater.* **1992**, *4*, 102; b) J. Guay, P. Kasai, A. Diaz, M. Wu, J. M. Tour, *Chem. Mater.* **1992**, *4*, 1097; c) J. Roncali, *Acc. Chem. Res.* **2000**, *33*, 147.
[16] R. J. Waltman, J. Bargon, *Tetrahedron* **1984**, *40*, 3963.
[17] J. Roncali, F. Garnier, R. Garreau, M. Lemaire, *Synth. Met.* **1986**, *15*, 323.
[18] G. Zotti, G. Schiavon, *Synth. Met.* **1990**, *39*, 183.
[19] Gaussian 98 (Revision A.9), M. J. Frisch, G. W. Trucks, H. B. Schlegel, G. E. Scuseria, M. A. Robb, J. R. Cheeseman, V. G. Zakrzewski, J. A. Montgomery, Jr., R. E. Stratmann, J. C. Burant, S. Dapprich, J. M. Millam, A. D. Daniels, K. N. Kudin, M. C. Strain, O. Farkas, J. Tomasi, V. Barone, M. Cossi, R. Cammi, B. Mennucci, C. Pomelli, C. Adamo, S. Clifford, J. Ochterski, G. A. Petersson, P. Y. Ayala, Q. Cui, K. Morokuma, D. K. Malick, A. D. Rabuck, K. Raghavachari, J. B. Foresman, J. Cioslowski, J. V. Ortiz, B. B. Stefanov, G. Liu, A. Liashenko, P. Piskorz, I. Komaromi, R. Gomperts, R. L. Martin, D. J. Fox, T. Keith, M. A. Al-Laham, C. Y. Peng, A. Nanayakkara, C. Gonzalez, M. Challacombe, P. M. W. Gill, B. G. Johnson, W. Chen, M. W. Wong, J. L. Andres, M. Head-Gordon, E. S. Replogle, J. A. Pople, Gaussian, Inc., Pittsburgh, PA, **1998**.
[20] a) P. Flükiger, H. P. Lüthi, S. Portmann, J. Weber, Molekel, Version 4.3, Swiss Center for Scientific Computing, Manno (Switzerland), **2000–2002**, http://www.cscs.ch/molekel/; b) S. Portmann, H. P. Lüthi, *Chimia* **2000**, *54*, 766.

Received: October 17, 2005
Published online: January 27, 2006

 © 2006 Wiley-VCH Verlag GmbH & Co. KGaA, Weinheim